Braz J Phys (2016) 46:334–340
DOI 10.1007/s13538-016-0407-6

SOCIEDADE BRASILEIRA DE FÍSICA
CrossMark

NUCLEAR PHYSICS

Analysis of ^{6}Li Scattering at 240 MeV Using Different Nuclear Potentials

A. H. Al-Ghamdi[1] · **Awad A. Ibraheem**[2,3]

Received: 23 January 2016 / Published online: 8 March 2016

Abstract Angular distributions of the elastic and inelastic scattering cross sections of ^{6}Li projectile on different heavy ion target nuclei including the ^{24}Mg, ^{28}Si, ^{48}Ca, ^{58}Ni, ^{90}Zr, and ^{116}Sn at energy of 240 MeV have been analyzed by using two different folded potentials based on the CDM3Y6 and São Paulo potentials for the real part of the optical potential, while the imaginary parts have a phenomenological Woods-Saxon shape. Coupled channel calculations for the low-lying 2^{+} state at 1.369, 1.779, 3.832, 1.454, 2.186, and 1.29 MeV for ^{24}Mg, ^{28}Si, ^{48}Ca, ^{58}Ni, ^{90}Zr, and ^{116}Sn, respectively, have been carried out, and the best fit values for *B*(EL) with the above models have been extracted by fitting the inelastic scattering cross section and compared with the values of previous works. The total reaction cross section and real and imaginary volume integrals have also been investigated.

Keywords Optical model · Elastic scattering · Folding potential

PACS · 25.70.Bc · 24.10.Ht · 27.20.+n

✉ A. H. Al-Ghamdi
aalghamdi5@kau.edu.sa

Awad A. Ibraheem
awad_ah_eb@hotmail.com

[1] Physics Department, Faculty of Science, King Abdulaziz University, Jeddah, Saudi Arabia

[2] Physics Department, King Khalid University, Abha, Saudi Arabia

[3] Physics Department, Al-Azhar University, Assiut Branch, Assiut 71524, Egypt

1 Introduction

The elastic and inelastic scattering of ^{6}Li ions has been extensively studied with different bombarding energies from various target nuclei. Chen et al. [1–3] studied elastic and inelastic scattering of 240-MeV ^{6}Li from ^{24}Mg, ^{28}Si, and ^{116}Sn. They investigated the experimental data by using the double-folding (DF) calculation method based on several nucleon-nucleon (NN) interactions. They found that *B*(EL) values are in agreement with electromagnetic results for low-lying states and also agree with giant resonance distributions obtained with α particles. They demonstrated successfully that the 240-MeV ^{6}Li scattering is a viable way to study the isoscalar giant monopole resonance (ISGMR) and the giant dipole resonance (ISGDR). Also, this can be useful particularly in rare isotope studies where ^{6}Li is used as the target. On the other hand, the differential cross sections of ^{6}Li + ^{24}Mg and ^{6}Li + ^{28}Si systems have attracted considerable interest because they exhibit two different structures: one is diffractive oscillations at forward angles while the other one is strongly refractive patterns at large angles. In a recent work, Kim et al. [4] used the tangential velocity at the distance of closest approach (r_c) within the framework of the eikonal model to reproduce the elastic cross section structure. Several studies used continuum discretized coupled channel (CDCC) techniques to confirm that the elastic scattering data can be fitted well with the potential renormalization close to one when coupling to the breakup channel is included. However, the elastic scattering of ^{6}Li found that the magnitude of the folded potential must be reduced by a renormalization factor (Nr ~ 0.5–0.6) to fit the data [5–8].

In the present work, we investigated the elastic and inelastic scattering of ^{6}Li projectile on the heavy ion (HI) targets: ^{24}Mg, ^{28}Si, ^{48}Ca, ^{58}Ni, ^{90}Zr, and ^{116}Sn [1–3, 9, 10]. The optical potential model is used to fit the data. We used two different folding models based on the CDM3Y6 and the São Paulo

potentials to construct the real part of the optical potential while phenomenological Woods-Saxon (WS) shape was considered for the imaginary part of the potential. Coupled channel calculations for the low-lying 2^+ state at 1.369, 1.779, 3.832, 1.454, 2.186, and 1.29 MeV for ^{24}Mg, ^{28}Si, ^{48}Ca, ^{58}Ni, ^{90}Zr, and ^{116}Sn, respectively, were carried out, and the best fit values for B(EL) with these models had been investigated. The paper is structured in the following way: after this introduction, a theoretical formalism is presented in Section 2, while the analysis of the elastic and inelastic scattering data using microscopic optical model potentials is described in Section 3, and finally, conclusions are summarized in Section 4.

2 Theoretical Formalism

The key inputs in a folding calculation are the nuclear densities of the interacting nuclei and the effective NN interaction. In the past, different NN effective interactions have been used in folding model calculations. In the present work, we used São Paulo (SP) potential and DF potential based on the CDM3Y6 interaction to carry out density-dependent DF calculations. The SP potential has been successful in describing the elastic scattering and peripheral reaction channels for a large number of HI systems in a wide energy regions, i.e., from sub-Coulomb to 200 MeV/nucleon. Also, it described successfully the total reaction and fusion cross sections for hundreds of systems [11–13]. In this model, for HI systems, the real part of the local-equivalent interaction is associated to the DF potential $V_F(R)$ through these two equations as

$$V_N(R,E) = V_F(R)e^{-\frac{4V^2}{C^2}} \tag{1}$$

$$V^2(R,E) = \frac{2}{\mu}[E - V_C(R) - V_N(R,E)] \tag{2}$$

where C is the speed of light, V is the local relative velocity between the two nuclei, and $V_C(R)$ is the Coulomb potential. The velocity dependence of the SP potential arises from the effects of the Pauli non-locality which can be obtained numerically by solving Eqs. (1) and (2) by an iterative process [11–13]. However, folding potentials depend on the matter densities of the nuclei involved in the collision

$$V_F(R) = \iint \rho_P(r_P)\rho_T(r_T)V_0\delta\left(\left(\left|\vec{s}\right|\right)\right)d^3r_P d^3r_T,\ \vec{s} = \vec{R} - \vec{r}_P + \vec{r}_T \tag{3}$$

where $\rho_P(r_P)$ and $\rho_T(r_T)$ are the nuclear matter density distributions of ^{6}Li and target nuclei, respectively with $V_0 = -456$ MeV fm^3.

For the sake of comparison, it may be useful to compare the SP potential with the DF one based upon the density-dependent effective NN interaction known as CDM3Y6. Then, the DF potential is defined as [14–16]

$$V_{\mathrm{CDM3Y6}}(R) = \iint \rho_P(r_P)\rho_T(r_T)\ \upsilon_{\mathrm{NN}}^{\mathrm{CDM3Y6}}(S,E,\rho)d^3r_P d^3r_T \tag{4}$$

In order to perform the folding calculation, Fermi distributions are used for the ground state of both projectile and target on the form

$$\rho(r) = \rho_0/\left(1 + \exp\left[\frac{r-c}{a}\right]\right) \tag{5}$$

The corresponding parameters ρ_0, C, and α together with the corresponding r.m.s. radii are given in Table 1. For more realistic consideration, we introduce the density and energy dependent factor $F(E,\rho)$ defined as

$$F(E,\rho) = g(E)C(1 + \alpha\exp(-\beta\rho)) - \gamma\rho, \tag{6}$$

where $g(E) = 1 - 0.003\ E/A$ with parameters adjusted to reproduce saturation properties of nuclear matter and to yield a nuclear incompressibility $K = 252$ MeV in the HF approximation [16], where $C = 0.2658$, $\alpha = 3.803$, $\beta = 1.4099$ fm^3, and $\gamma = 4.0$ fm^3.

The explicit form for the direct and exchange parts of this interaction are expressed as given in Refs. [14, 15]. The direct (exchange) part is defined as

$$\upsilon_{\mathrm{NN}}^{\mathrm{CDM3Y6}}(S,E,\rho) = F(E,\rho)\upsilon_{\mathrm{nn}}^{D(\mathrm{EX})} \tag{7}$$

where

$$\upsilon_{\mathrm{NN}}^{D}\left(\left|\vec{s}\right|\right) = 11062\frac{e^{-4\left|\vec{s}\right|}}{4\left|\vec{s}\right|} - 2538\frac{e^{-2.5\left|\vec{s}\right|}}{2.5\left|\vec{s}\right|} \tag{8}$$

Table 1 Parameters of the nuclear matter densities of ^{6}Li, ^{24}Mg, ^{28}Si, ^{48}Ca, ^{58}Ni, ^{90}Zr, and ^{116}Sn for the Fermi model of the ground state used in the folding calculations

Density	ρ_0 (fm^{-3})	c (fm^{-2})	α(fm)	$\langle r_T^2\rangle^{1/2}$ (fm)	Ref
^{6}Li	0.1993	1.5080	0.500	2.193	[3]
^{24}Mg	0.1704	2.995	0.478	2.922	[2]
^{28}Si	0.175	3.150	0.475	3.012	[2]
^{48}Ca	0.1870	3.723	0.515	3.479	[9]
^{58}Ni	0.1760	4.080	0.515	3.695	[10]
^{90}Zr	0.1647	4.90	0.515	4.251	[10]
^{116}Sn	0.1540	5.490	0.515	4.664	[3]

and the knock-on exchange part in the finite-range form as

$$\upsilon_{NN}^{Ex}\left(\left|\vec{s}\right|\right)=-1524\frac{e^{-4\left|\vec{s}\right|}}{4\left|\vec{s}\right|}-518.8\frac{e^{-2.5\left|\vec{s}\right|}}{2.5\left|\vec{s}\right|}-7.847\frac{e^{-0.7027\left|\vec{s}\right|}}{0.7027\left|\vec{s}\right|} \quad (9)$$

The derived potentials are obtained by using the modified momentum space folding DFPOT and DFPD4 computer codes [17].

3 Results and Discussion

It is customary in optical model analysis to employ the WS form for the real and imaginary potentials. This WS potential has six (or more) free parameters form. The total nucleus-nucleus potential for the optical model calculation can be written as

$$U(r)=-V_0\left[1+\exp\left(\frac{r-R_V}{a_0}\right)\right]^{-1}-iW_0\left[1+exp\left(\frac{r-R_I}{a_I}\right)\right]^{-1}+V_C(R_C) \quad (10)$$

The radii have the forms $R_V=r_v(A_P^{1/3}+A_T^{1/3})$, $R_I=r_I(A_P^{1/3}+A_T^{1/3})$ with mass number of the projectile (target) $A_P(A_T)$. The Coulomb potential $V_C(R_C)$ for a point charge interacting with a uniformly charged sphere of radius $R=1.25(A_P^{1/3}+A_T^{1/3})$ fm is considered. In our calculations, the real part of the DF potentials has been considered for the optical model analysis of the data as described in Eqs. (1) and (4) instead of the real part of WS as in Eq. (10) while the imaginary parts $W(R)$ are kept

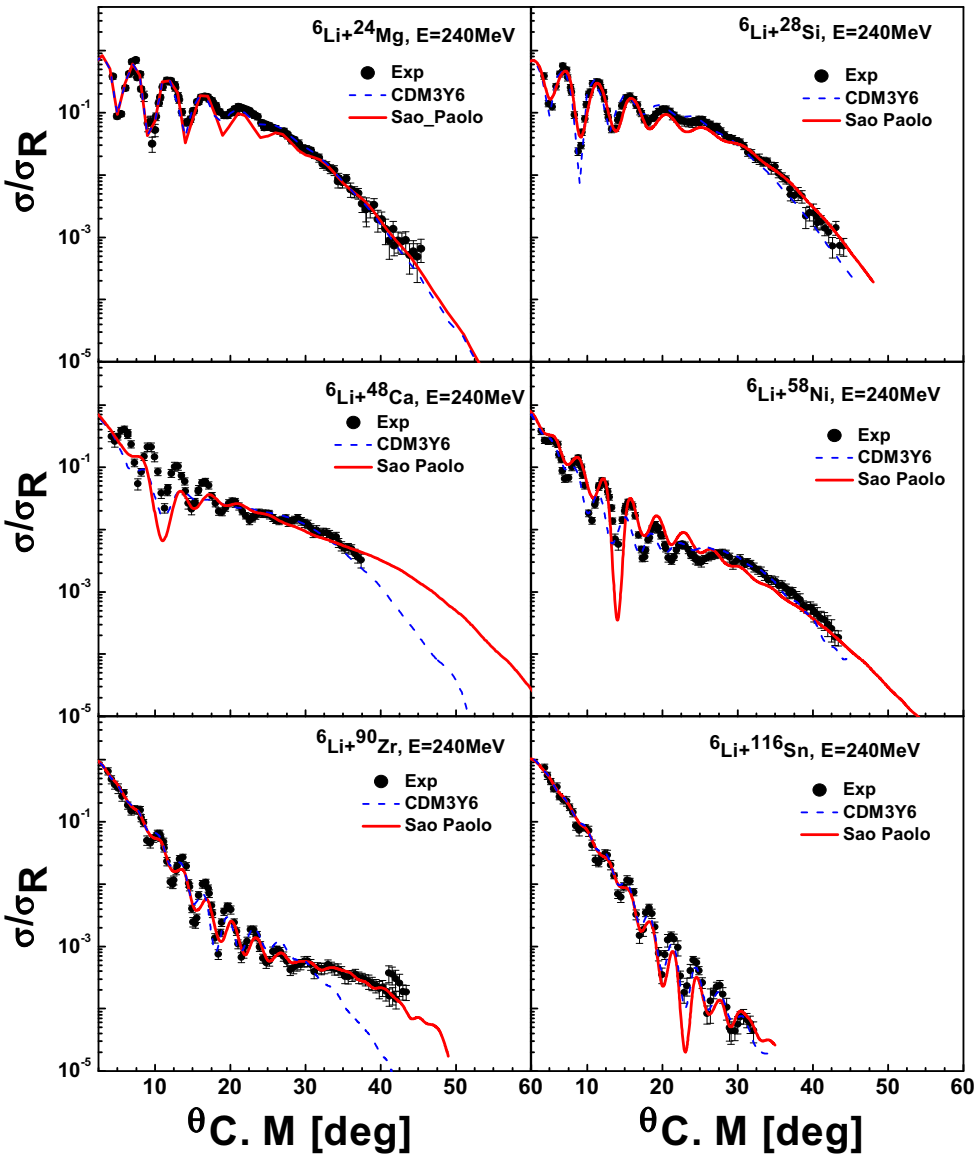

Fig. 1 Experimental angular distribution of the cross section (relative to Rutherford cross section) and fits for ^{6}Li projectile on the different HI of targets including the ^{24}Mg, ^{28}Si, ^{40}Ca,^{58}Ni, ^{90}Zr, and ^{116}Sn elastic scattering using SP and CDM3Y6 potential parameters as shown in Table 2. The *error bars* indicate statistical and systematic errors

in the WS form. Then, the total nucleus-nucleus potential used in the optical model calculation is

$$U(R) = N_R V(R) + i\, W(R) + V_C(R_C) \tag{11}$$

where N_R is a renormalization factor for the real folding potential. The computer code HIOPTIM94 [18] is used to calculate the angular distributions of the elastic scattering differential cross section. An automatic search routine is carried out to vary the parameters of this potential by optimizing the real renormalization factor N_R for the calculated potentials besides the three parameters of the imaginary phenomenological WS potentials, i.e., the depth W_0, radius r_I, and diffuseness a_I. The quality of fitted data over the experimental results has been estimated by χ^2, which is defined by

$$\chi^2 = \frac{1}{N}\sum_{i=1}^{N}\left[\frac{\sigma_{\mathrm{cal}}(\theta_i)-\sigma_{\mathrm{exp}}(\theta_i)}{\Delta\sigma_{\mathrm{exp}}(\theta_i)}\right]^2 \tag{12}$$

where $\sigma_{\mathrm{cal}}(\theta_i)$ and $\sigma_{\mathrm{exp}}(\theta_i)$ are, respectively, the calculated and experimental values of elastic scattering differential cross section at angle θ_i and $\Delta\sigma_{\mathrm{exp}}(\theta_i)$ is the corresponding experimental error, while N is the number of data points. The obtained angular distributions for the elastic scattering of ^{6}Li from ^{24}Mg, ^{28}Si, ^{48}Ca, ^{58}Ni, ^{90}Zr, and ^{116}Sn at energy 240 MeV as a ratio with the Rutherford cross section are displayed in Fig. 1. The data are fitted using the constructed two different folding potentials. The corresponding best fit potential parameters are listed in Table 2 together with the volume integrals as well as chi-squares and total reaction cross sections.

As a test, the optical parameters obtained from elastic scattering and inelastic scattering data from excitations of well-known low-lying states in ^{24}Mg, ^{28}Si, ^{48}Ca, ^{58}Ni, ^{90}Zr, and ^{116}Sn were compared to coupled channel calculations with these parameters using the CHUCK3 code [19] as shown in Fig. 2. Coupled channel calculations for ^{6}Li inelastic scattering to the low-lying 2^+ state of the considered targets are carried out with transition potentials obtained by the deformed potential model. In the deformed potential model calculations, both the real and imaginary parts of the transition potentials are obtained by taking the first derivatives of the calculated potentials. The mass deformation parameters for the 2^+ states are obtained from electromagnetic B(EL) values by assuming that the mass and Coulomb deformation lengths are the same. B(EL) values are extracted by fitting the inelastic scattering cross sections. As shown in Table 3, the obtained values are comparable to the adopted values of the previous work (http://nrv.jinr.ru/nrv/webnrv/map/nucleus.php?q=Mg24&Z=12&A=24).

Since the target nuclei are deformed, it is essential to treat their collective excitation explicitly in the framework of the coupled channel calculations. It has been assumed that the target nucleus has a static quadrupole deformation.

Table 2 Optical potential parameters obtained from our best fit to the experimental data at $E = 240$ MeV using the HIOPTIM94 code [18]

Pot.	N_R	W_0 MeV	r_w fm	a_w fm	J_R MeVfm^3	J_I MeVfm^3	σ_R mb	σ_R [Ref]	χ^2	Rs
^{6}Li + ^{24}Mg										
DF(R)	0.992	39.425	0.9748	1.0005	280.76	162.95	1742.0	1680 [2]	6.2	6.49
SP(R)	1.0	46.256	0.9826	0.8600	288.62	178.07	1584.0	–	9.37	6.32
^{6}Li + ^{28}Si										
DF(R)	0.852	40.235	0.9536	1.0303	278.56	148.15	1818.0	1650 [2]	9.33	6.65
SP(R)	0.953	40.734	0.9884	0.8528	274.58	147.13	1596.0	–	11.9	6.38
^{6}Li + ^{48}Ca										
DF(R)	0.783	37.566	0.9890	1.1830	245.80	126.20	2449.0	2021 [9]	10.9	7.89
SP(R)	1.028	51.240	0.9601	0.960	287.90	142.20	2098.0	–	4.89	7.21
^{6}Li + ^{58}Ni										
DF(R)	0.70	39.657	0.9747	1.1906	221.20	118.26	2554.0	2187 [10]	25.40	8.03
SP(R)	1.030	75.474	0.9272	0.8958	291.30	171.22	2149.0		19.90	7.64
^{6}Li + ^{90}Zr										
DF(R)	0.663	22.932	1.2264	0.9120	208.43	93.23	2865.0	2709 [10]	19.9	8.98
SP(R)	0.852	38.652	1.0454	1.1253	240.51	110.14	2950.0		7.01	8.64
^{6}Li + ^{116}Sn										
DF(R)	0.653	28.952	0.8547	0.9284	207.34	96.03	3079.0	2885 [3]	5.99	9.43
SP(R)	0.830	58.623	0.9901	1.1332	234.96	132.17	3251.0		9.70	9.51

The volume depth (W_0) in MeV and radius and diffuseness parameter (r_I and a_I, respectively) in fm. Real and imaginary volume integrals (J_R and J_I) in MeVfm^3, total reaction cross section(σ_R) in mb and the best fit χ^2. The last column shows the strong absorption radius Rs

Hence, its rotation can be described using the collective rotational model. Therefore, it is taken into account by deforming the real part of the optical potential in the following way

$$R(\theta,\varnothing) = r_0\left(A_P^{(1/3)} + A_T^{(1/3)}\right)\left(1 + \beta_2 Y_{20}(\theta,\varnothing)\right) \qquad (13)$$

where β_2 is the deformation parameter and $\delta = \beta_2 R$ is the deformation length. These β_2 values needed to fit the magnitude of 2^+ data. The invariant parameter in the calculations is in fact the deformation length or its value derived from the reduced electromagnetic transition probability B(EL) rather than β_2 itself (http://nrv.jinr.ru/nrv/webnrv/map/nucleus.php?q=Mg24&Z=12&A=24).

For the coupled channel calculations, also δ_λ^m may be determined from normalizing the intrinsic quadrupole moment Q_{20} by

$$\left(\frac{16\pi}{(2\lambda+1)}\right)^{\frac{1}{2}} \int_0^\infty \rho_t(r_{tr}) r_T^{\lambda+2} \mathrm{d}r_T = \frac{A_t}{(Z_t)} Q_{20} \qquad (14)$$

In the present calculations, the first two excited states of the target nuclei are included and the coupling scheme is employed. The code CHUCK3 [19] is used for all inelastic scattering calculations. The results for the ground and excited states, shown in Fig. 2, are very close to the experimental data. The magnitude of the cross sections and the phase of the oscillations are obtained correctly at most of angles as evident from the last column of Table 2. These analyses also revealed

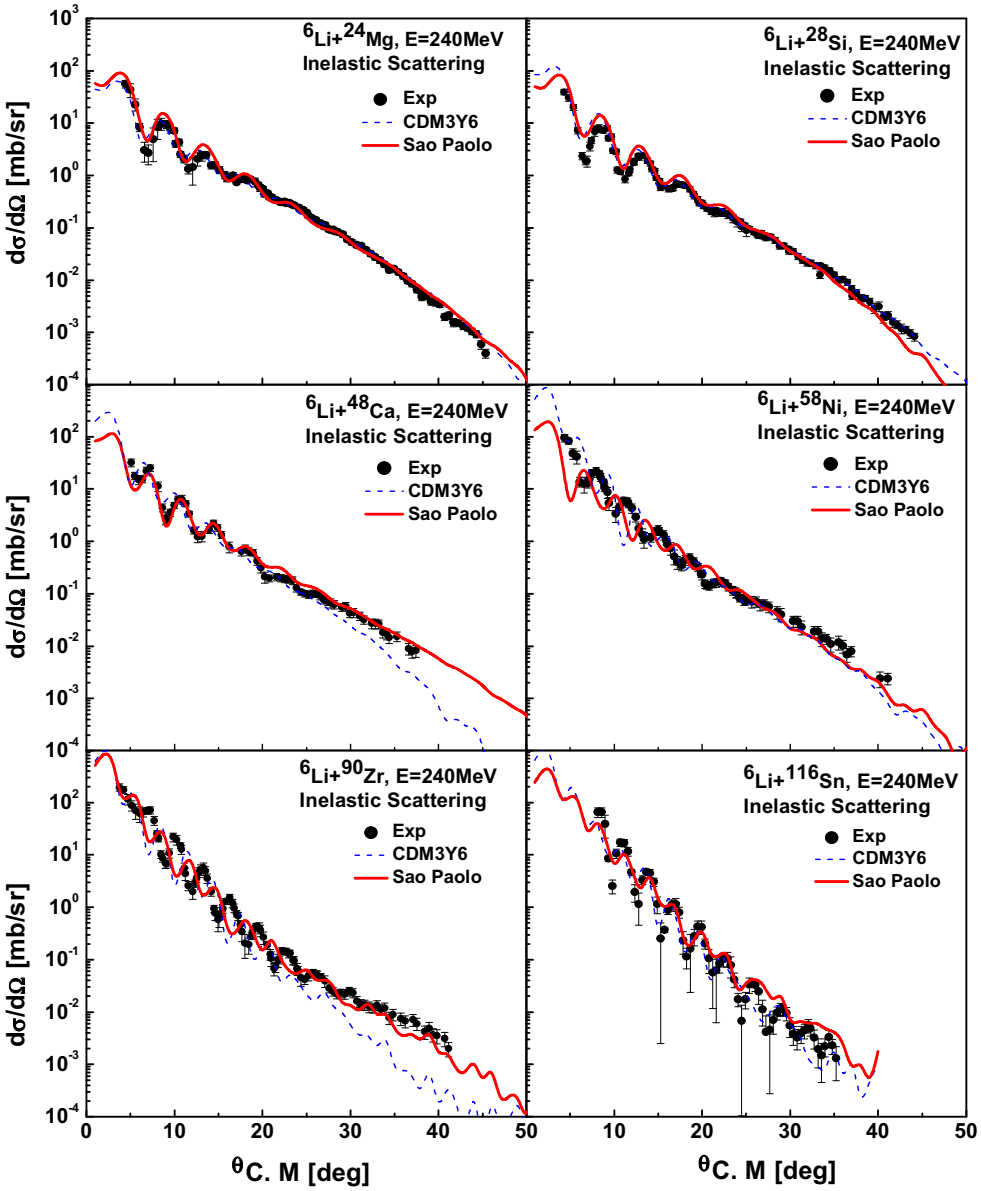

Fig. 2 The angular distributions of the differential cross sections for inelastic scattering to the 2+ state for ^{6}Li projectile on the different HI of targets including the ^{24}Mg, ^{28}Si, ^{40}Ca,^{58}Ni, ^{90}Zr, and ^{116}Sn elastic scattering using SP and CDM3Y6 potential parameters shown in Table 2 along with the data points are plotted versus average center of mass angle. The *error bars* indicate statistical and systematic errors

Table 3 The best fit B(EL) values of $J^{\pi}=2^{+}$, for the ^{24}Mg, ^{28}Si, ^{48}Ca, ^{58}Ni, ^{90}Zr, and ^{116}Sn obtained with CDM3Y6 and SP Potentials. Adopted values of B(EL) as well as values extracted from previous in addition to the intrinsic quadruple moment Q_{20}, are shown

Nucleus	Model	β_2	$B(E2)$ e^2 fm^4	Q_{20} fm
^{24}Mg	SP	0.38	334.66	58.0
$J^{\pi}=2^{+}$,	CDM3Y6	0.28	181.7	42.7
$E_x=1.369$ MeV	Ref. [2]		465.0	
	Adopted value	0.605	432 ± 11	65.9
^{28}Si	SP	0.31	355.80	59.81
$J^{\pi}=2^{+}$,	CDM3Y6	0.33	375.40	61.4
$E_x=1.779$ MeV	Ref. [2]		311.0	
	Adopted value	0.407	326 ± 12	57.2
^{48}Ca	SP	0.084	89.24	29.96
$J^{\pi}=2^{+}$,	CDM3Y6	0.11	142.5	37.8
$E_x=3.832$ MeV	Ref. [9]		116.0	
	Adopted value	0.106	95 ± 3.2	30 ± 5
^{58}Ni	SP	0.15	610.0	78.31
$J^{\pi}=2^{+}$,	CDM3Y6	0.14	704.6	84.2
$E_x=1.454$ MeV	Ref [10].		662.0	
	Adopted value	0.1826	695 ± 20	83.6 ± 12
^{90}Zr	SP	0.072	599.20	77.61
$J^{\pi}=2^{+}$,	CDM3Y6	0.07	779.5	88.5
$E_x=2.186$ MeV	Ref. [10]		590.0	
	Adopted value	0.0894	610 ± 40	78.3 ± 26
^{116}Sn	SP	0.10	2213.6	149.20
$J^{\pi}=2^{+}$,	CDM3Y6	0.12	2375.13	154.50
$E_x=1.29$ MeV	Ref. [3]		2330	
	Adopted value	0.1118	2090 ± 60	144.9 ± 21

that the data are sensitive to the optical potential in the surface region. Satchler [20] pointed out that scattering equivalent potential as determined in the vicinity of the strong absorption radius R_{SA} is defined as

$$R_{SA}=1.5\left(A_P^{(1/3)}+A_T^{(1/3)}\right)\text{fm} \quad \text{or} \quad R_{SA}=1.1\left(A_P^{1/3}+A_T^{1/3}\right)+2.5\ \text{fm} \tag{15}$$

The most significant remark by Satchler [21] is that one should not assume that one can obtain a unique potential or set of phase shifts even with data of high quality in the presence of weak absorption. On the other hand, one may investigate the mass dependence of the volume integral of the imaginary part of optical potentials (J_I), defined as:

$$J_I=\frac{1}{A_P A_T}\int W(R)d\vec{R} \tag{16}$$

This quantity is currently used as a sensitive measure of the potential strength where $W(R)$ is the imaginary part of the optical potential, as shown in Table 2. It is found that the J_I decreases as the target mass increases. This result is in agreement with those of Ref. [9].

On the other hand, the extracted values of the reaction cross section, σ_R, from the present analysis using the derived folded potentials, are 1663 ± 11, 1707 ± 157, 2273.5 ± 248, 2351.5 ± 286, 2907.5 ± 60, and 3165 ± 121 mb for ^{4}Mg, ^{28}Si, ^{48}Ca, ^{58}Ni, ^{90}Zr, and ^{116}Sn, respectively. Unfortunately, there are no experimental values for σ_R which can be compared with the values obtained by our calculations. However, the extracted values are quite consistent with those theoretically calculated recently by many authors [1–4, 9, 10] using different microscopic optical model analyses as well as WS potential.

4 Conclusions

In view of the above results, we can conclude that the elastic scattering differential cross section for ^{6}Li at 240 MeV can be qualitatively reproduced with the two choices of the DF model based on the CDM3Y6 and SP potentials. To test further the optical potential parameters, the B(EL) values for low-lying states have been extracted. The number of their peaks, magnitudes, and positions agrees well with the experimental data for both considered folding potentials. The choice of the WS form for the imaginary part of the potential is more appropriate than assuming that it is proportional to its real part. In general, we observed a good agreement between our calculations and the experimental data for both the elastic and inelastic angular distributions. This is an additional confirmation of the SP potential to describe the inelastic scattering data successfully.

Acknowledgments We thank Dr. A. Khan and Dr. M. Aygun for carefully reading the paper and Professor M. El-Azab Farid for useful communications. This work was supported by the Deanship of Scientific Research (DSR), King Abdulaziz University, Jeddah, under grant no. (D1435-535-130). The authors, therefore, gratefully acknowledge the DSR technical and financial support.

References

1. X. Chen, Y.-W. Lui, H.L. Clark, Y. Tokimoto, D.H. Youngblood, Phys. Rev. **C79**, 024320 (2009)
2. X. Chen, Y.-W. Lui, H.L. Clark, Y. Tokimoto, D.H. Youngblood, Phys. Rev. **C80**, 014312 (2009)
3. X. Chen, Y.-W. Lui, H.L. Clark, Y. Tokimoto, D.H. Youngblood, Phys. Rev. **C76**, 054606 (2007)
4. K. Yong Joo, W. Jong-Kwan, L. Seok Jae, J Korean Phys. Soc **60**, 1477 (2012)
5. Y. Sakuragi, Phys. Rev. C **35**, 2161 (1987)
6. Y. Sakuragi, M. Ito, Y. Hirabayashi, C. Samanta, Prog. Theor. Phys. **98**, 521 (1997)
7. M. Aygun, I. Boztosun, K. Rusek, Mod. Phys. **A28**, 1350112 (2013)

8. M. El-Azab Farid, A.A. Ibraheem, J.H. Al-Zahrani, W.R. Al-Harbi, M.A. Hassanain, J. Phys. **G40**, 075108 (2013)
9. Krishichayan, X. Chen, Y.-W. Lui, J. Button, D.H. Youngblood, Phys. Rev. **C81**, 044612 (2010)
10. Krishichayan, X. Chen, Y.-W. Lui, Y. Tokimoto, J. Button, D.H. Youngblood, Phys. Rev. **C81**, 014603 (2010)
11. L.C. Chamon, D. Pereira, M.S. Hussein, M.A. Cândido Ribeiro, D. Galetti, Phys. Rev. Lett. **79**, 5218 (1997)
12. L.C. Chamon, D. Pereira, M.S. Hussein, Phys. Rev. **C58**, 576 (1998)
13. L.C. Chamon, Nucl. Phys. **A787**, 198c (2007)
14. G.R. Satchler, W.G. Love, Phys. Rep. **55**, 183 (1979)
15. G. Bertsch, J. Borysowicz, H. McManus, W.G. Love, Nucl. Phys. **A284**, 399 (1977)
16. D.T. Khoa, G.R. Satchler, Nucl. Phys. **A668**, 3 (2000)
17. J. Cook, Comput. Phys. Commun. **25**, 215 (1982); D.T. Khoa, (unpublished).
18. N. M. Clarke, HI-OPTIM code, University of Birmingham, UK (unpublished).
19. P. D. Kunz, Coupled-channels computer code CHUCK3 (unpublished).
20. G.R. Satchler, Nucl. Phys **A279**, 493 (1977)
21. G.R. Satchler, Nucl. Phys **A574**, 575 (1994)